Journal of Applied Polymer Science

# Systematic Investigation on Parameters of Solution Blown Micro/Nanofibers using Response Surface Methodology Based on Box-Behnken Design

**Huiqing Lou,[1] Wentao Li,[2] Chulin Li,[1] Xinhou Wang[1,3]**

[1]College of Textiles, Donghua University, Shanghai 201620, China

[2]Department of Radiology, Cancer Center, Fudan University, Shanghai 200032, China

[3]Key Laboratory of Science and Technology of Eco-Textiles, Ministry of Education, Donghua University, Shanghai 201620, China

*Correspondence to*: X. Wang (E-mail: xhwang@dhu.edu.cn).

**ABSTRACT:** Response surface methodology, based on the four-factor, three-level Box-Behnken design, has been utilized to facilitate a more systematic understanding of the solution and processing parameters of solution blown polyethylene oxide (PEO) micro/nanofibers. The factors investigated include air pressure, solution concentration, nozzle diameter, and injection rate. Fiber diameters, ranging from 137 to 1982 nm, are associated with these variables by applying a response surface model. The linear coefficients of air pressure and solution concentration, the interactive effect between air pressure and injection rate as well as the quadratic terms of nozzle diameter and injection rate are demonstrated statistically significant. Verification of the response surface model is successfully accomplished. Consequently, this study puts forward an overview of the effect of solution and technical parameters on solution blown submicron PEO fibers and provides a train of thought for fabricating other micro/nanofibers. © 2013 Wiley Periodicals, Inc. J. Appl. Polym. Sci. 130: 1383–1391, 2013

**KEYWORDS:** nanostructured polymers; manufacturing; theory and modeling; synthesis and processing; fibers

Received 27 December 2012; accepted 24 March 2013; Published online 25 April 2013

**DOI: 10.1002/app.39317**

## INTRODUCTION

Nanofiber manufacturing techniques have attracted much attention in academic and industrial field in recent years, on account of nanofibers possessing extraordinary structure features, novel performance and exhibiting tremendously potential application.[1–3] Nanofibers can be obtained via various methods such as drawing, self-assembly, phase separation, template synthesis, bicomponent spinning, flash spinning, melt blowing, and electrospinning, just to name a few.[1,2,4] It is worth mentioning that great efforts have been made to perfect the structure, quality as well as property of nanofibers, raise yields and cut costs of electrospinning and other nanofiber manufacturing technologies, comprising incorporating critical principles of traditional textile fiber processing methods with nanotechnology.[5] Those emerging alternative techniques include gas-assisted spinning including electroblowing,[6,7] gas-jet/electrospinning,[8,9] solution blowing,[10–19] and gas jet process,[20] centrifugal spinning[5] involving centrifugal electrospinning and centrifugal nanospinning, and various modification of needleless spinning,[21–23] etc. In the above methods, solution blowing methods have prominent production efficiency as well as flexibility, and are particularly suitable for fabricating nanofibers from barely electrospinnable polymer materials with higher solution viscosity[6] or lower permittivity,[10] additionally, less easily melt blown polymers with higher melt point/viscosity or sensitive to heat degradation.[11]

Solution blowing is named relatively to melt blowing and is inspired by melt blowing, but it is generally capable of manufacturing fibers with high speed pressured gas, and it integrates the advantages of electrospinning producing fibers from a few micrometers down to several nanometers as well as melt blowing scalable for commercial production. To date, several studies have been accomplished in solution blowing process to preliminarily investigate the principle of fiber formation and effect of processing parameters on fiber morphology and to explore the application of solution blown fibers. The feasibility and effectiveness has been elaborated by solution blowing several polymer solution such as poly(methyl methacrylate) (PMMA), polystyrene, poly(lactic acid) (PLA) and polyaniline. The diameters of different polymers varied from 40 nm to several micrometers, and fibers could be directly collected on biological tissue.[10] Ultrafine polyvinylpyrrolidone was generated by feeding polymer solution to a die assembly similar to that used in conventional melt blowing, and process parameters were investigated by single factorial experiment.[11] PMMA and PAN core-

shell nanofibers has been co-blown as well as made into mesoscopic carbon tubes,[12] coupled with solution blown monolithic and core-shell nanofibers containing soy protein,[16] and then solution blown three-dimensional carbon fiber nonwovens was employed in microbial fuel cells, promising a great potential in the case of sustainable energy supply and handling.[13] The high-surface-area PAN-based activated carbon was prepared by solution blowing and evaluated as $CO_2$ adsorption in a flue gas stream.[14] Nanocomposite fibrous membranes comprising of multiwalled carbon nanotubes and PLA were fabricated by solution blowing method and subsequently applied to platforms for glucose biosensors.[17,18] Submicron-scale cellulose fibers were also successfully solution blown by raising the air temperature along the spinning line.[19]

Development of useful applications requires a thorough knowledge of the parameters of the solution blowing process and their effect on final products. Despite the extensive and rapid growth of interest in solution blowing, the effects of the solution properties and process parameters are still under study theoretically and experimentally.[10,11,15] Response surface methodology (RSM) is a collection of statistical and mathematical techniques beneficial for developing, improving, and optimizing process,[24] which is capable of statistical investigation on single-factor and interactive effects synchronously,[25] and enables reduced number of experimental runs that provides sufficient information for statistically acceptable results as compared to full-factorial experiments.[26] This approach complies with a sequential order including screening the independent variables and corresponding levels, constructing surface model by a proper and right experimentally design method, estimating the coefficients of the fitted approximation model as well as assessing the adequacy and validity of the surface model.[27] Sukigara et al.[28] reported RSM was used in situations where several variables influence a feature (called the response) of the system, and it enabled to obtain the surface contours of these parameters that outlined the processing window and pointed out the direction to attain the optimum condition in the form of an Eigen value. Oliveira et al.[15] preliminarily discussed the response surface of average diameter as a function of polymer concentration and feed rate at a constant air pressure, and found that the polymer concentration played an important role on fiber diameter ranging from 70 to 2000 nm as well as fiber distribution.

In this article, RSM was performed to identify and quantify the significance of solution properties (especially concentration) and process parameters (air pressure, nozzle diameter, and injection rate) that influenced fiber morphology especially diameter, and confirmed the experimental design range available for a subsequent optimization. In view of the favorable characteristics of precise prediction overall the factor space, Central Composite design (CCD) and Box-Behnken design (BBD) are generally recommended as experimental design methods. The BBD is a three evenly spaced levels design, and for a second-order response model with three or more factors, the BBD procedure possesses even more advantages than CCD for, such as less run number of design points coupled with rotatable and spherical design.[24,27] The objective of this article was to construct a BBD-based response surface model to evaluate the statistical significance of the preferred parameters under consideration, to predict and optimize the solution blown fiber diameter.

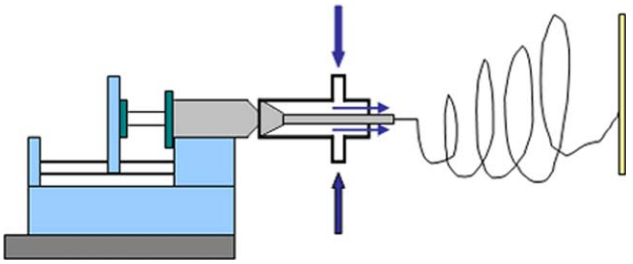

**Figure 1.** Schematic of the solution blowing apparatus. [Color figure can be viewed in the online issue, which is available at wileyonlinelibrary.com.]

## EXPERIMENTAL

### Materials

Polyethylene oxide (PEO average MW ~ 1,000,000) was purchased from Liansheng Chemical (China) and used without further purification. PEO solution with different wt % concentration was prepared by dissolving the PEO powder in the distilled water, and then stirred in the heat water bath at room temperature.

### Preparation of Solution Blown Fibers

The schematic of the solution blowing system was depicted in Figure 1. The main components of the setup were a syringe pump (LSP01-1A, Baoding Longer Precision Pump Co., Ltd., China), a home-made annular concentric nozzle and a compressed air source. The syringe pump was used to supply the polymer solution at the required injection rate. An air blowing system was attached to the dual spinneret. The blown air was generated by an oil-less compressor (DA7002, Jiangsu Dynamic Medical Technology, China) and the air pressure was controlled by the air-operated precision regulator. It was worth noting that the first (inner) nozzle was protruded from the concentric second (outer) nozzle about 4 mm. The distance from the tip of the first nozzle to the collector was 50 cm. The solution blowing process was conducted by continuously delivering the PEO solution to the first nozzle, which was surrounded by the pressured high velocity air supplied through the annular channel. The emerging polymer solution jet was then accelerated and stretched by the surrounding air flow. During the process, the solvent evaporated and the polymer fibers deposited on the copper wire mesh collector.

The morphology of the solution blown PEO fibers was observed by a scanning electron microscopy (SEM, Hitachi TM-1000), after being gold-coated under vacuum to lessen charge assembling. The average fiber diameter was determined by analyzing the images with an image processing software (Image J, National Institutes of Health, USA), and 30 fibers were randomly selected to obtain the average fiber diameter.

### Experimental Design and Statistical Analysis

A standard RSM design called BBD was performed to investigate and identify the relationship between the fiber diameter and processing variables. The BBD is well suited to fit a quadratic surface, which is usually designed for process optimization.

**Table I.** Independent Variables and their Levels in the Box-Behnken Experimental Design

| Factors | Codes | Variable levels and range | | |
|---|---|---|---|---|
| | | −1 | 0 | +1 |
| Air pressure (kgf/cm$^2$) | A | 0.125 | 0.25 | 0.375 |
| Solution concentration (wt %) | B | 8 | 9 | 10 |
| Nozzle diameter (mm) | C | 0.41 | 0.63 | 0.84 |
| Injection rate (mL/h) | D | 0.5 | 1.0 | 1.5 |

The four independent variables were air pressure (A), solution concentration (B), nozzle diameter (C), and injection rate (D). The average diameter of the fibers observed from each experiment was used as the response value. Each variable was coded at three levels: −1, 0 and +1. These levels were laid out equally spaced. The factors and their corresponding levels (coded and actual) chosen in the four-factor-three-level BBD were shown in Table I. The ranges of the variables were selected from preliminary one-factor-at-a-time experiments, which found that fibers could be produced in the solution blowing process when factors A, B, C, and D were about 0.125–0.375 kgf/cm$^2$, 8–10 wt %, 0.41–0.84 mm, and 0.5–1.5 mL/h, respectively. Thus, 29 experiments including five center points were conducted in a randomizing run order to reduce impact of variation on response values owing to the external factors.

The design points and experiment data (Table II) were analyzed by means of RSM to fit a full second-order polynomial equation. The typical quadratic response surface model for four factors was fitted as follows:

$$Y = \beta_0 + \sum_{i=1}^{4} \beta_i X_i + \sum_{i=1}^{4} \beta_{ii} X_i^2 + \sum_{i=1}^{3} \sum_{j=i+1}^{4} \beta_{ij} X_i X_j + \xi \qquad (1)$$

where $Y$ is the response value. $X_i$ is the independent variable. $\beta_0$, $\beta_i$, $\beta_{ii}$, and $\beta_{ij}$ are the regression coefficient of the intercept, linear, squared, and interaction terms. $\xi$ is the random error term.

The fitness of the full quadratic approximation of the BBD response surface model was estimated by the analysis of variance (ANOVA) and various *R*-Squared ($R^2$) values. In statistics, *F*-value, the test statistic of ANOVA or *F*-test, is used to test the significance of adding new model terms to those terms already in the model; and *P*-value is also a measure of statistical significance.[24] The *F*-values and relevant *P*-values ("Prob > *F*") were used to examine the significance of each source of terms (linear, two-factor interaction, and quadratic) and the regression coefficients of the fitted model. It is generally understood that the conventional use of the 0.05 significance level as the maximum acceptable probability for determining statistical significance was established,[29] terms with their probability (*P*-value) falling below 0.05 at the 95% confidence interval were identified as statistical significance.[24,26] A multiple regression analysis (Least square method) was employed to fit the response value and the experiment data. Model reduction was carried out to further refine full quadratic response surface model by clicking off the insignificant terms with a significance level greater than 5% ($P > 0.05$). $R^2$, the coefficient of multiple determination, represents the proportion of the response variation interpreted by the model, in other words, it indicates how adequately the quadratic model fits the data. The value of $R^2$ is between 0 and 1.0. A low $R^2$ value implies that there is other variation around the mean prediction. To an adequate approximation, a value of $R^2$ larger than 0.9 is typically desirable.[30] However, $R^2$ is very sensitive to the degree of freedom and always increases as we add terms to the model, so the adjusted $R^2$ ($R^2_{adj}$) was chosen as well, which is much less sensitive to the degrees of freedom and cannot be affected seriously by including more terms in the model, whereas it is always lower than $R^2$.[30] And a reasonable agreement is that the $R^2_{adj}$ and predicted $R^2$ ($R^2_{pred}$) values should be within 0.2 of each other.

**Table II.** Arrangement and Response Values of the Four-Variable-Three-Level Box-Behnken Design

| Exp. no. | Coded independent variable levels | | | | Response value Average fiber diameter (nm) |
|---|---|---|---|---|---|
| | A | B | C | D | |
| 1 | 0 | 0 | −1 | 1 | 767.98 |
| 2 | 1 | 1 | 0 | 0 | 719.33 |
| 3 | −1 | −1 | 0 | 0 | 617.58 |
| 4 | 1 | 0 | 0 | 1 | 772.99 |
| 5 | −1 | 0 | 0 | −1 | 680.28 |
| 6 | 0 | 0 | 1 | 1 | 901.97 |
| 7 | −1 | 1 | 0 | 0 | 875.65 |
| 8 | 0 | 1 | −1 | 0 | 977.73 |
| 9 | 0 | 0 | −1 | −1 | 653.02 |
| 10 | 0 | 0 | 0 | 0 | 720.41 |
| 11 | 1 | 0 | 1 | 0 | 771.90 |
| 12 | 0 | −1 | 0 | 1 | 597.04 |
| 13 | 0 | 0 | 0 | 0 | 727.19 |
| 14 | 1 | −1 | 0 | 0 | 465.57 |
| 15 | 0 | 0 | 0 | 0 | 710.26 |
| 16 | 0 | 0 | 0 | 0 | 717.88 |
| 17 | 0 | 1 | 0 | −1 | 712.00 |
| 18 | 0 | 0 | 1 | −1 | 784.72 |
| 19 | 1 | 0 | −1 | 0 | 800.86 |
| 20 | 0 | 0 | 0 | 0 | 711.78 |
| 21 | −1 | 0 | −1 | 0 | 938.53 |
| 22 | 0 | −1 | −1 | 0 | 579.39 |
| 23 | 1 | 0 | 0 | −1 | 369.82 |
| 24 | −1 | 0 | 0 | 1 | 700.49 |
| 25 | 0 | 1 | 0 | 1 | 862.18 |
| 26 | 0 | −1 | 0 | −1 | 480.72 |
| 27 | 0 | 1 | 1 | 0 | 1084.04 |
| 28 | 0 | −1 | 1 | 0 | 689.60 |
| 29 | −1 | 0 | 1 | 0 | 1007.81 |

**Table III.** Analysis of Variance (ANOVA) for Response of the Fitted Full Quadratic Polynomial Model

| Source | SS | DF | MS | *F*-value | *P*-value |
|---|---|---|---|---|---|
| Model | 6.75E + 05 | 14 | 48201.22 | 17.22 | < 0.0001 [a] |
| *Regression* | | | | | |
| A | 70,513.40 | 1 | 70,513.40 | 25.20 | 0.0002 [a] |
| B | 2.70E + 05 | 1 | 2.70E + 05 | 96.59 | < 0.0001 [a] |
| C | 22,753.13 | 1 | 22,753.13 | 8.13 | 0.0128 [a] |
| D | 70,854.16 | 1 | 70,854.16 | 25.32 | 0.0002 [a] |
| AB | 4.64 | 1 | 4.64 | 1.66E − 03 | 0.9681 |
| AC | 2412.77 | 1 | 2412.77 | 0.86 | 0.3689 |
| AD | 36,664.59 | 1 | 36,664.59 | 13.10 | 0.0028 [a] |
| BC | 3.80 | 1 | 3.80 | 1.36E − 03 | 0.9711 |
| BD | 286.62 | 1 | 286.62 | 0.10 | 0.7537 |
| CD | 1.31 | 1 | 1.31 | 4.68E − 04 | 0.9830 |
| A^2 | 754.36 | 1 | 754.36 | 0.27 | 0.6117 |
| B^2 | 2167.89 | 1 | 2167.89 | 0.77 | 0.3936 |
| C^2 | 1.34E + 05 | 1 | 1.34E + 05 | 47.94 | < 0.0001[a] |
| D^2 | 27,815.13 | 1 | 27,815.13 | 9.94 | 0.0071 [a] |
| Residual | 39,178.06 | 14 | 2798.43 | | |
| Pure Error | 187.64 | 4 | 46.91 | | |
| Cor Total | 7.14E + 05 | 28 | | | |

SS, sum of square; DF, degree of freedom; MS, mean square; *P*-value, a statement describing *F*.
[a] Values are statistically significant (at 5% level of significance).

To diagnose the statistical properties of the selected model, the characteristic of residuals was analyzed. The residuals were defined as the diversity between the predicted values and the actual experimental data at the same factor levels in the whole design space under discussion. For an adequate prediction model, the residuals are desired to comply with a normal distribution, which means the deviation between predicted values and the actual experimental outcomes are generated in random sequence.[24,27,31] In this study, normal probability plot of the residuals was checked. The normal probability plot indicates whether the residuals follow a normal distribution, in which case the data points should be approximately linear. It is noteworthy unless the leverages of all runs in a design are identical, the standard errors of the residuals are different. That means the raw residuals belong to distinct normal populations. As a consequence, raw residuals fail to check the regression assumption. Fortunately, studentizing the residuals makes all different normal distribution to a single standard normal distribution, on account of studentized residuals counterbalancing diverse weight because of the design point position.

## RESULTS AND DISCUSSION

### Model Development for Fiber Diameter

Submicron-scale PEO fibers were well fabricated at each design point of the four factors [air pressure (kgf/cm$^2$), solution concentration (wt %), nozzle diameter (mm), and injection rate (mL/h)] three levels ( − 1, 0 and + 1) BBD experiment, which is a robust response surface design method. The results were shown in Table II; the average diameter of the fibers from each run was measured and specified as the response value.

According to the statistical theory, the experiment data were used to fit a full quadratic response surface model equation. A statistical analysis of variance (ANOVA) of the experiment was implemented to evaluate the model. The ANOVA results (Table III) suggested that the full second-order model was statistically significant (at 5% level of significance). Table III also indicates that the linear terms such as air pressure, solution concentration, nozzle diameter, and injection rate (A, B, C, and D) showed significant effects ($P < 0.05$). Besides the linear source, two of the quadratic terms $C^2$ and $D^2$, as well as the interaction coefficient AD also indicated statistically significant effects on the mean fiber diameter at 5% level of significance.

The full quadratic polynomial model was not adopted because of several insignificant terms in the model. A backward model reduction method was utilized and insignificant effects ($P > 0.05$) were removed from the model. The backward method is recognized as the most preferred option for model reduction algorithm because all model terms will be recalculated to give another chance to be included in the model. The regression coefficients with their relevant *P*-values of the reduced quadratic model were recomputed by means of a multiple regression analysis (Table IV). The $R^2$, "$R^2_{adj}$", and "$R^2_{pred}$" values were, respectively, 0.9378, 0.9171, and 0.8679, particularly, the "$R^2_{pred}$" of 0.8679 was in reasonable consistency with the "$R^2_{adj}$"of 0.9171. The "Adeq Precision" measures the signal to noise ratio, which greater than 4 is desirable. In this study, the

**Table IV.** Estimated Coefficients of the Refined Surface Model

| Source | Coefficient | DF | Standard error | *F*-value | *P*-value |
|---|---|---|---|---|---|
| Intercept | 701.65 | 1 | 13.87 | | |
| A | −76.66 | 1 | 13.28 | 33.34 | < 0.0001 [a] |
| B | 150.09 | 1 | 13.28 | 127.80 | < 0.0001 [a] |
| C | 43.54 | 1 | 13.28 | 10.76 | 0.0036 [a] |
| D | 76.84 | 1 | 13.28 | 33.50 | < 0.0001 [a] |
| AD | 95.74 | 1 | 22.99 | 17.34 | 0.0004 [a] |
| C^2 | 148.43 | 1 | 17.51 | 71.90 | < 0.0001 [a] |
| D^2 | −60.86 | 1 | 17.51 | 12.09 | 0.0023 [a] |

ratio of 26.999 confirmed an adequacy of signal, and the model can be applied to navigate the consequent design space. The refined model consisted of a series of significant terms and can be proposed as below:

$$Y = 617.77 - 2145.09X_1 + 150.09X_2 - 3811.33X_3 + 257.60X_4 + 1531.84X_1X_4 + 3211.09X_3^2 - 243.44X_4^2 \quad (2)$$

where $Y$ is the average fiber diameter (nm). $X_i$ ($i$ = 1, 2, 3, 4) is the actual independent variable, $X_1$ is the air pressure (kgf/cm$^2$), $X_2$ is the solution concentration (wt %), $X_3$ is the nozzle diameter (mm), and $X_4$ is the injection rate (mL/h).

Equation (2) implies that the air pressure and solution concentration exhibit a direct correlation with the average diameter, whereas the nozzle diameter and injection rate show the quadratic relationship with the mean fiber diameter. Besides, the air pressure and injection rate demonstrate an interactive effect on the average diameter.

### Response Surface Analysis

The three-dimensional (3D) surface plots of the response variable (average fiber diameter) as a function of the selected factors (two-factors-at-a-time) were demonstrated in Figure 2(a–f). The 3D surface plots, showing the graphical display of the fitted regression model, were shaped by combining points of identical response values (identical fiber diameter).

**Solution Blown Fiber Diameter: Air Pressure Dependence.** The influence of air pressure on solution blown fiber morphology was illustrated in Figure 2(a–c). The impact of air pressure on average fiber diameter was constrained by the solution concentration to a certain extent [Figure 2(a)]. At low polymer concentration (8–9 wt %), increasing air pressure had insignificant effect on reducing fiber diameter, whereas at high concentration (10 wt %), the enlargement of air pressure slightly decreased the fiber diameter. This observation revealed some similarity to the investigation of voltage effect on electrospun fiber,[32] as shown in this article, the diameter was not remarkably varied with changing applied voltage and the influence of voltage was diminished when the polymer solution was low. The effect of air pressure on fiber diameter was suggested to be independent from the nozzle diameter [Figure 2(b)], as at whatever nozzle diameter, adding air pressure had a trend of diminishing fiber diameter first and then slightly enhancing fiber diameter. It was obvious that no relevant interactive term between air pressure and nozzle diameter existed in the fitted model. The decrease of fibers diameter with increasing air pressure was more apparent especially at low injection rate within the spinnable range as shown in Figure 2(c). This could be attributed to low mass flow per unit time undergoing the larger stretching action. As stated earlier, there was a strong interaction effect between air pressure and injection rate in the refined surface model.

**Solution Blown Fiber Diameter: Solution Concentration Dependence.** Figure 2(a,d,e) depicts the effect of solution concentration on average fiber diameter. Given the air pressure or injection rate at a certain value, the average fiber diameter increased monotonously with concentration rising, and accordingly lower solution concentration brought forth smaller fiber diameters visibly, as demonstrated in Figure 2(a,e). It was in good consistence with the earlier study on solution blowing and electrospinning process,[10,11,15,33] which also suggested that fiber diameter was responsive to the varied solution concentration. As the concentration was raised, the viscosity of the polymer solution increased because of more molecular chain entanglement, hence, the forces of viscosity and surface tension controlled by the viscoelastic property of polymer fibers gone up correspondingly. The higher viscoelastic force was prone to suppress the stretching and shearing force during the solution blowing process. Consequently, thicker fibers were produced. Figure 2(a,e) also indicates that thinner fibers could be obtained theoretically by lowering solution concentration below 8 wt %, whereas this was not feasible experimentally. In the course of our study, we had found PEO solution with concentration below 8 wt % such as 6 wt % could not be spun into fibers other than droplets and beads. So the empirical model and the contour plots should not be extrapolated.

On the other side, as shown in Figure 2(d), varying solution concentration within the processable range would lead to thinner fiber diameter, and higher concentration coupled with larger nozzle diameter benefited the formation of fibers with smaller diameter. This result was probably similar with the previous observation on electrospun PEO/water system,[34] which had found that there was a binomial distribution of fiber diameter spun from higher concentration solutions (> 8 wt %), and a second population of smaller diameters (about one third of those in the primary population) occupied a considerable percentage of the whole number of fibers. However, the underlying reason behind this result was ambiguous, and other experiments with the high speed videography would be carried out to validate and explain this observation in our future research.

**Solution Blown Fiber Diameter: Nozzle Diameter Dependence.** The effect of altering the nozzle diameter on fiber diameter was investigated as revealed in Figure 2(b,d,f). In the normal course of events, enlarging the nozzle diameter would reduce the friction force per unit volume between the inner wall of nozzle and the polymer solution, and the larger nozzle diameter provided more basis points for multi-jet ejection because of the higher polymer solution flow volume and the bigger pendent

Applied Polymer SCIENCE

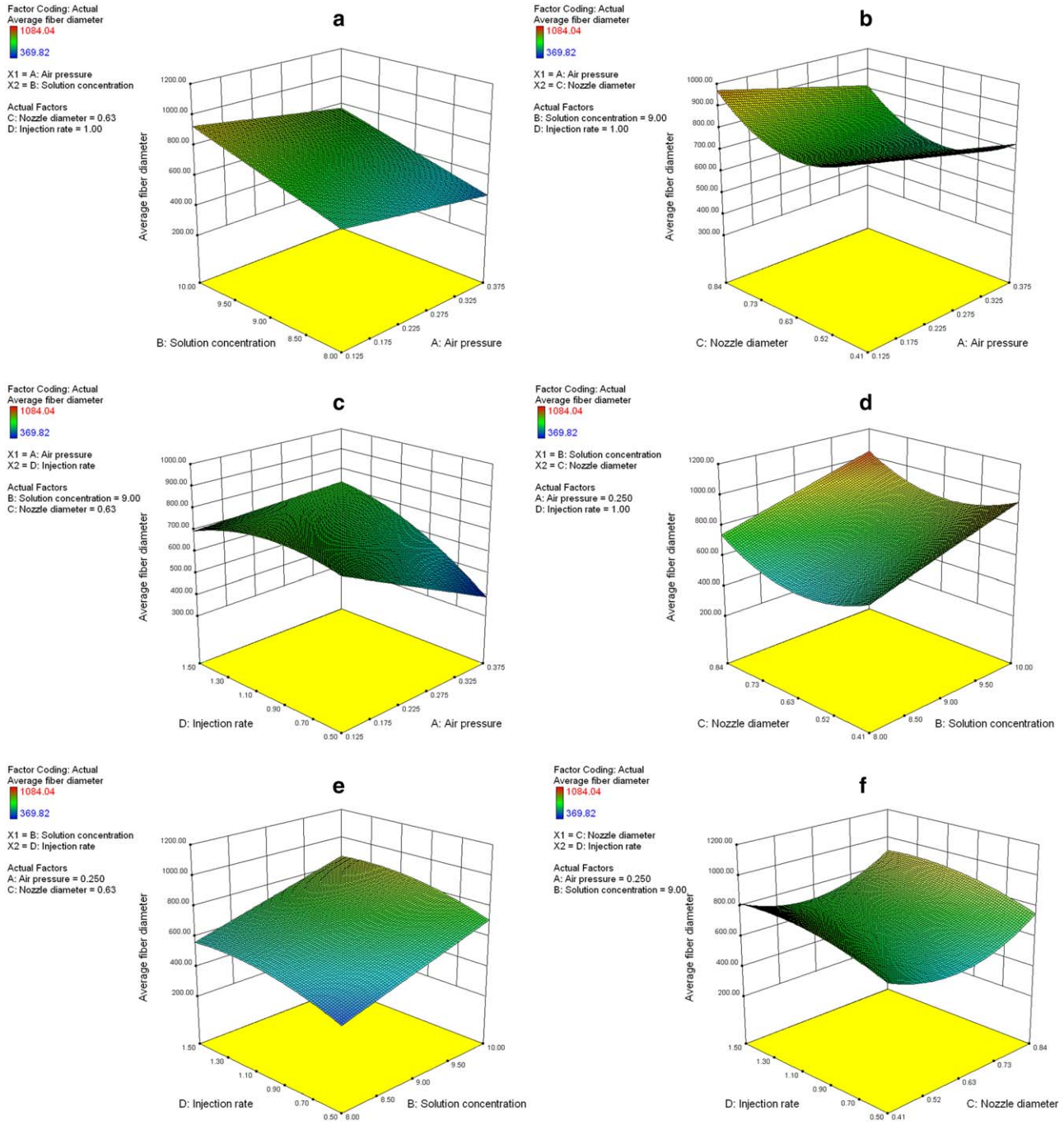


**Figure 2.** 3D surface plots of the response variable (average fiber diameter) as a function of the selected factors (two-factors-at-a-time) : (a) Air pressure and Solution concentration (nozzle diameter = 0.63 and injection rate = 1.00), (b) air pressure and nozzle diameter (solution concentration = 9.00 and injection rate = 1.00), (c) air pressure and injection rate (solution concentration = 9.00 and nozzle diameter = 0.63), (d) solution concentration and nozzle diameter (air pressure = 0.250 and injection rate = 1.00), (e) solution concentration and injection rate (air pressure = 0.250 and nozzle diameter = 0.63), (f) nozzle diameter and injection rate (air pressure = 0.250 and solution concentration = 9.00). [Color figure can be viewed in the online issue, which is available at wileyonlinelibrary.com.]

droplet. As a consequence, the fiber became thinner with the improving the nozzle size [Figure 2(d,f)], which bore some resemblance to Kong's research on electrospun PVA polymer solution.[35,36] However, the observation was different from the earlier research on electrospun P(LLA-CL) nanofiber,[37] which indicated that a thinner needle diameter led to bead-free fibers and no clogging at the needle tip, and the beads might be formed because of the boundary condition such as needle diameter. But a larger nozzle diameter coupled with a lower air pressure produced thicker fibers [Figure 2(b)], because the lower

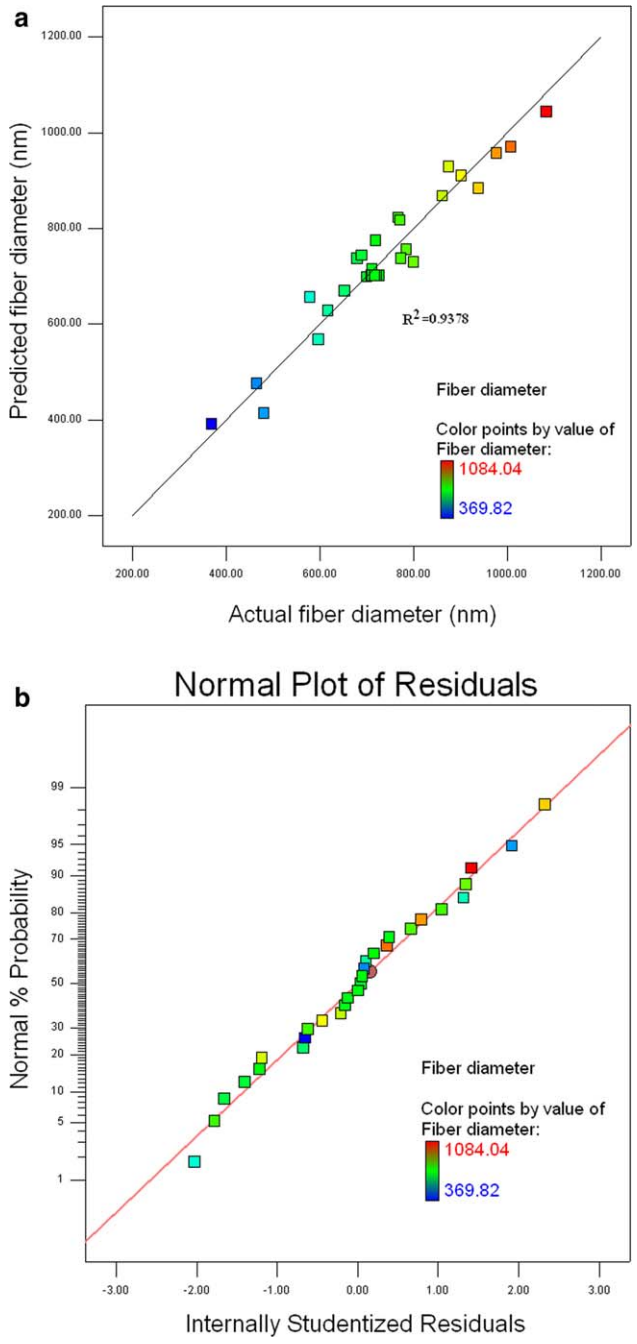


**Figure 3.** Assement of the accuracy of the response surface model. (a) Plot of model predicted fiber diameters against experimental values. (b) Normal probability plot of the studentized residuals. [Color figure can be viewed in the online issue, which is available at wileyonlinelibrary.com.]

pressure brought about weaker applied force on the bigger droplet at the tip of the needle.

**Solution Blown Fiber Diameter: Injection Rate Dependence.** A certain amount of solution suspended at the tip of the nozzle was required for the purpose of keeping the dynamically balanced Taylor cone[38] and bringing forth a consecutive jet. In addition, solution injection rate played a decisive role in the solution quantity applicable to fiber forming.[2] In this article, the impact of solution volume injection rate was exhibited in Figure 2(c,e,f)). As mentioned above, the minimum injection rate combined with the higher air pressure yielded the smaller diameter fibers in the processing window [Figure 2(c)], which was corresponded to the fitted surface model. Compared with the parameter like solution concentration, the fiber diameter was not responsive to the change of injection rate [Figure 2(e)], as with previously investigated on electrospinning process,[32] the diameter of the electrospun fiber was not significantly changed with varied injection rate. It was worth noting that improving the injection rate and nozzle diameter would reduce the fibers diameter [Figure 2(f)], since the bottom of the nascent Taylor cone was equivalent to the nozzle diameter,[39] in other words, the pendant drop volume increased with larger size nozzle. Therefore, the shear force acting on the drop surface mounted because of the larger contact area between the air stream and jet flow.[7]

### Validation of the Response Surface Model

To evaluate the adequacy of the fitted regression model, the observed fiber diameters were compared with the predicted values [Figure 3(a)] and a linear correlation coefficient was calculated. It could be perceived that the predicted values were well in line with the actual experimental outcome. And a linear correlation coefficient of 0.9378 also indicated a valid correlation between the experimental data and the theoretically predicted values within the design space.

The probability plot of the studentized residuals was demonstrated [Figure 3(b)] to check off normality assumption. The plot indicated the normality in the error term, as the residuals were approximately linear. The normal probability distribution of residuals confirmed that the variation of model predicted values from the experimental consequences was random (no systematic bias).[27]

The prediction capability of the RSM model was validated by conducting additional three independent experiments, the predicted values were compared with the experimental results as

**Table V.** Validation of Model Prediction Against Experimental Outcomes for Factors under Consideration

| Exp. no. | Air pressure (kgf/cm$^2$) | Solution concentration (wt %) | Nozzle diameter (mm) | Injection rate (mL/h) | Fiber diameters (nm) | |
|---|---|---|---|---|---|---|
| | | | | | Experimental | Predicted |
| 1 | 0.18 | 8 | 0.63 | 0.8 | 586.22 | 576.58 |
| 2 | 0.20 | 8.7 | 0.84 | 0.5 | 785.32 | 779.89 |
| 3 | 0.36 | 10 | 0.63 | 1.2 | 843.79 | 860.15 |

shown in Table V, the experimentally observed values were in good accordance with the estimated responses. It should be mentioned that the model was available only under the present research conditions enumerated in this article and would require to be improved for any other polymer systems and solution blown conditions.

## CONCLUSIONS

A response surface model based on the BBD technique was constructed to investigate the relationship between the solution blown fiber diameters and processing parameters coupled with solution concentration, to optimize the experimental process and to predict fiber diameter. The response of RSM method indicated that solution blown parameters like air pressure, solution concentration, nozzle diameter, and injection rate had significant effect on the average fiber diameter. The interactive effect between air pressure and injection rate was also observed. Solution concentration demonstrated a direct impact on fiber diameter irrespective of air pressure or injection rate at the medium nozzle diameter. The lower injection rate coupled with the higher air pressure produced the smaller fiber diameter. The solution blown fiber diameter had a trend to decrease with nozzle diameter increasing. The predicted fiber diameters were in good agreement with the diameters observed experimentally. Verification experiments validated the accuracy of the refined surface model that proved to be an effective method for manufacturing fibers with tunable and predictable average fiber diameters. This study has shown that investigation of the solution concentration and process variables could lead to the possibility of tailoring the solution blown fiber morphology especially diameter.

## ACKNOWLEDGMENTS

Financial support from the Fundamental Research Funds for the Central Universities (NO. 12D10146) was highly appreciated.

## REFERENCES

1. Huang, Z. M.; Zhang. Y. Z.; Kotaki, M.; Ramakrishna, S. *Compos. Sci. Technol.* **2003**, *63*: 2223.
2. Ramakrishna, S.; Fujihara, K.; Teo, W. E.; Lim, T. C.; Ma, Z. An Introduction to Electrospinning and Nanofibers; World Scientific Pub Co Inc: Singapore, **2005**; Chapter 1, p 7.
3. Greiner, A.; Wendorff, J. H. *Angew. Chem. Int. Ed.* **2007**, *46*, 5670.
4. Nayak, R.; Padhye, R.; Kyratzis, I. L.; Truong, Y. B.; Arnold, L. *Text. Res. J.* **2012**, *82*, 129.
5. Luo, C. J.; Stoyanov, S. D.; Stride, E.; Pelan, E. *Chem. Soc. Rev.* **2012**, *41*, 4708.
6. Um, I. C.; Fang, D. F.; Hsiao, B. S.; Okamoto, A.; Chu, B. *Biomacromolecules* **2004**, *5*, 1428.
7. Kong, C.; Yoo, W.; Lee, K.; Kim, H. *J. Mater. Sci.* **2009**, *44*, 1107.
8. Yao, Y. Y.; Zhu, P. X.; Ye, H.; Niu, A. J.; Gao, X. S.; Wu, D. C. *Acta Polym. Sin.* **2005**, *687*.
9. Zhmayev, E.; Cho, D.; Joo, Y. L. *Polymer* **2010**, *51*, 4140.
10. Medeiros, E. S.; Glenn, G. M.; Klamczynski, A. P. Orts.; W. J.; Mattoso, L. H. C. *J. Appl. Polym. Sci.* **2009**, *113*, 2322.
11. Zhang, L.F.; Kopperstad, P.; West, M.; Hedin, N.; Fong, H. *J. Appl. Polym. Sci.* **2009**, *114*, 3479.
12. Sinha-Ray, S.; Yarin, A. L.; Pourdeyhimi, B. *Carbon* **2010**, *48*, 3575.
13. Chen, S. L.; Hou, H. Q.; Harnisch, F.; Patil, S. A.; Carmona-Martinez, A. A.; Agarwal, S.; Zhang, Y.Y.; Sinha-Ray, S.; Yarin, A. L.; Greiner, A.; Schroder, U. *Energy. Environ. Sci.* **2011**, *4*, 1417.
14. Hsiao, H. Y.; Huang, C. M.; Hsu, M. Y.; Chen, H. *Sep. Purif. Technol.* **2011**, *82*, 19.
15. Oliveira, J, E.; Moraes, E. A.; Costa, R. G. F.; Afonso, A. S.; Mattoso, L. H. C.; Orts, W. J.; Medeiros, E. S. *J. Appl. Polym. Sci.* **2011**, *122*, 3396.
16. Sinha-Ray, S.; Zhang, Y. Y.; Yarin, A. L.; Davis, S. C.; Pourdeyhimi, B. *Biomacromolecules* **2011**, *12*, 2357.
17. Oliveira, J. E.; Mattoso, L. H. C.; Medeiros, E. S.; Zucolotto, V. *Biosensors* **2012**, *2*, 70.
18. Oliveira, J. E.; Zucolotto, V.; Mattoso, L. H. C.; Medeiros, E. S. *J. Nanosci. Nanotechnol.* **2012**, *12*, 2733.
19. Zhuang, X. P.; Yang, X.C.; Shi, L.; Cheng, B. W.; Guan, K.T.; Kang, W. M. *Carbohydr. Polym.* **2012**, *90*, 982.
20. Benavides, R. E.; Jana, S. C.; Reneker, D. H. *ACS Macro Lett.* **2012**, *1*, 1032.
21. Yarin, A. L.; Zussman, E. *Polymer* **2004**, *45*, 2977.
22. Forward, K. M.; Rutledge, G. C. *Chem. Eng. J.* **2012**, *183*, 492.
23. Tang, S.; Zeng, Y. C.; Wang, X. H. *Polym. Eng. Sci.* **2010**, *50*, 2252.
24. Myers, R. H.; Montgomery, D. C.; Anderson-Cook, C. M. Response Surface Methodology: Process and Product Optimization using Designed Experiments; Wiley: New York, **2009**; Vol. *705*, Chapter 2, p 58.
25. Agarwal, P.; Mishra, P.; Srivastava, P. *J. Mater. Sci.* **2012**, *47*, 4262.
26. Neo, Y. P.; Ray, S.; Easteal, A. J, Nikolaidis, M. G.; Quek, S Y. *J. Food. Eng.* **2012**, *109*, 645.
27. Ray, S.; Lalman, J. A. *Chem. Eng. J.* **2011**, *169*, 116.
28. Sukigara, S.; Gandhi, M.; Ayutsede, J.; Micklus, M.; Ko, F. *Polymer* **2004**, *45*, 3701.
29. Cowles, M.; Davis. C. *Amer. Psychol.* **1982**, *37*, 553.
30. Tsimpliaraki, A.; Svinterikos, S.; Zuburtikudis, I.; Marras, S. I.; Panayiotou, C. *Ind. Eng. Chem. Res.* **2009**, *48*:4365.

31. Box, G. E. P.; Draper, N. R. Empirical Model-Building and Response Surfaces; Wiley: New York, **1987**; Chapter 7–13, p 205.

32. Tan, S. H.; Inai, R. Kotaki, M.; Ramakrishna, S. *Polymer* **2005**, *46*, 6128.

33. Hsiao, H. Y.; Huang, C .M.; Liu, Y. Y.; Kuo, Y. C.; Chen, H. *J. Appl. Polym. Sci.* **2012**, *124*, 4904.

34. Deitzel, J. M, Kleinmeyer, J.; Harris, D.; Beck Tan, N. C. *Polymer.* **2001**, *42*, 261.

35. Kong, C. S.; Lee, T. H.; Lee, K. H.; Kim, H. S. *J. Macromol. Sci. Part B Phys.* **2009**, *48*, 77.

36. Kong, C. S.; Lee, S. G.; Lee, S. H.; Lee, K. H.; Noh, H. W.; Yoo, W. S.; Kim, H. S. *J. Macromol. Sci. Part B: Phys.* **2011**, *50*, 528.

37. Mo, X. M.; Xu, C. Y.; Kotaki, M.; Ramakrishna, S. *Biomaterials* **2004**, *25*, 1883.

38. Zong, X. H.; Kim K, Fang, D. F.; Ran, S. F.; Hsiao, B. S.; Chu, B. *Polymer* **2002**, *43*, 4403.

39. Katti, D. S.; Robinson, K. W.; Ko, F. K.; Laurencin, C. T. *J Biomed Mater Res Part B: Appl. Biomater.* **2004**, *70B*, 286.